Computational Medical Physics Working Group Workshop II, Sep 30 – Oct 3, 2007
University of Florida (UF), Gainesville, Florida USA on CD-ROM, American Nuclear Society, LaGrange Park, IL (2007)

HDRK-MAN: A WHOLE-BODY VOXEL MODEL BASED ON HIGH-RESOLUTION COLOR SLICE IMAGES OF A KOREAN ADULT MALE CADAVER

Chan Hyeong Kim*, Sang Hyoun Choi, and Jong Hwi Jeong
Department of Nuclear Engineering
Hanyang University
17 Haengdang-dong, Seongdong-gu, Seoul 133-791, Korea
chkim@hanyang.ac.kr; sh524mc@hanmail.net; jonghwi@hanyang.ac.kr

Choonsik Lee
Department of Nuclear and Radiological Engineering
University of Florida
Gainesville, FL 32611, USA
choonsiklee@gmail.com

Min Suk Chung
Department of Anatomy
Ajou University School of Medicine
San 5 Wonchon-dong, Yeongtong-gu, Suwon 443-749, Korea
dissect@madang.ajou.ac.kr

ABSTRACT

A Korean voxel model, named ‘High-Definition Reference Korean-Man (HDRK-Man),’ was constructed using high-resolution color photographic images that were obtained by serial sectioning the cadaver of a 33-year-old Korean adult male. The body height and weight, the skeletal mass, and the dimensions of the individual organs and tissues, were adjusted to the Reference Korean data. The resulting model was then implemented into a Monte Carlo particle transport code, MCNPX, to calculate the dose conversion coefficients for the internal organs and tissues. The calculated values, overall, were reasonable in comparison with the values from other adult voxel models. HDRK-Man showed higher dose conversion coefficients than other models, due to the facts that HDRK-Man has a smaller torso and that the arms of HDRK-Man are shifted backward. The developed model is believed to adequately represent the average Korean workers and thus can be used for more accurate calculation of dose conversion coefficients for the Korean workers in the future.

KEYWORDS: Voxel model; Tomographic model; Monte Carlo; Dosimetry; Organ Dose

1. INTRODUCTION

Many different anthropomorphic computational models have been developed in the radiation protection and medical communities to calculate the dosimetric quantities for human body exposed to radiation. Simple geometric forms such as spheres, slabs, and cylinders were initially used to represent the human body, and subsequently more complicated heterogeneous models, called 'MIRD (Medical Internal Radiation Dose)' or stylized models, were introduced for more realistic representation [1].

The first MIRD-type model defined the human body and internal organs with relatively simple mathematical expressions in the forms of planes, cylinders, cones, spheres, and ellipsoids, and with only three media: skeleton, soft tissue, and lung [2]. The MIRD-type model was then followed by many similar models, including pediatric models at various ages, gender-specific adult models, and a pregnant adult female model [3-5]. The MIRD-type models practically have been used as the standard computational representations of the ICRP Reference Man [6] in the radiation protection community. It is obvious, however, that the anatomical structure of the human body, which is very complicated, cannot be accurately described by simple surface equations, resulting in significant errors in organ dose calculations especially for the cases of internal radiation exposure. To that end, the International Commission on Radiological Protection (ICRP) recently decided, for the purpose of the forthcoming updates of dose conversion coefficients for organ doses and effective doses, to use voxel models in place of the conventional MIRD-type models [7].

The voxel model, also called the 'tomographic model,' first reported by Gibbs *et al*. [8] in 1984, was used to calculate effective doses for dental radiology examinations. The first model was the representation of the head and torso from computed tomography (CT) of a female cadaver. Zubal *et al*. [9] constructed an adult male model from the CT data of an adult male patient of dimensions similar to the Reference Man data in ICRP 23 [6]. Dimbylow [10] constructed an adult male model called NORMAN from the whole-body magnetic resonance (MR) images of a healthy volunteer. The voxel resolution was scaled in order to match the height and weight of the segmented model to the ICRP 23 reference data [6]. More recently, Zankl *et al*. [11] and Schlattl *et al*. [12] adjusted the dimensions of the previously constructed adult male and female models, Golem and Laura, to the reference values in ICRP 89 [13] and 70 [14]. The adjustment was fairly comprehensive, including the body height and weight, the skeletal mass, and the dimensions of individual organs and tissues. The developed models, which were named 'Rex' and 'Regina', have been adopted by the ICRP as reference phantoms for the forthcoming updates of the dose conversion coefficients for workers and adult members of the public [12].

Acknowledging the anatomical and physical differences between the different racial groups, Saito *et al*. [15] constructed a Japanese voxel model Otoko by segmenting the whole-body CT images of a patient whose external dimensions were in good agreement with the Japanese Reference Man data [16]. Meanwhile, several Korean voxel models were also constructed in Korea, by Lee *et al*. [17], using MR and CT images. The KTMAN-2 model, the most recent model, was constructed using the CT images of a 35-year-old healthy adult male volunteer. The volunteer had a height and weight of 172 cm and 68 kg, which are close to the Reference Korean data for male (171 cm, 68 kg) [18]. The developed model is 172 cm in height and 66.8 kg in weight, having a voxel resolution of 2 mm $\times$ 2 mm $\times$ 5 mm.

In general, CT and MR images provide fairly good information for accurate delineation of organs, but it is difficult to delineate some organs accurately if they are of similar material composition (e.g., ovaries, pancreas, oesophagus, adrenals, and thymus) or in continuous movement (e.g., gastro-intestines and heart) [19]. Consequently, the segmentation process involves significant subjective decisions that can impair the integrity of the resulting model. In fact, it has been reported that "the uncertainties associated with organ masses will be [on the] order of 10% or more" [19]. Xu *et al*. [20] constructed a high-resolution voxel model, called VIP-Man, based on color photographic slice images of a cadaver of a 38-year-old male. VIP-Man, which has the voxel resolution of 0.33 mm $\times$ 0.33 mm $\times$ 1 mm, is known to be the most complete body description so far. The model, however, is of only limited value for use in radiation protection, in that it represents a relatively large person (186 cm in height and 103 kg in weight), which is a significant deviation from the ICRP reference data (176 cm and 73 kg), and even more of a deviation from the Reference Korean data (171 cm and 68 kg).

This paper describes the construction of a high-quality Korean voxel model, named 'High-Definition Reference Korean-Man (HDRK-Man),' which was constructed using high-resolution color photographic slice images obtained by serial sectioning the cadaver of a 33-year-old Korean adult male. The dimensions, including the body height and weight, the skeletal mass, and those of the individual organs and tissues, were adjusted to the Reference Korean data [18] according to the procedure followed in the construction of the ICRP reference phantoms, Rex and Regina [12]. The model was implemented into a general purpose Monte Carlo particle transport code, MCNPX [21], to calculate the dose conversion coefficients for four idealized photon irradiation geometries: antero-posterior (AP), postero-anterior (PA), right-lateral (RLAT), and left-lateral (LLAT). The results were then compared with the reported values from other computational models, that is, one Korean voxel model, KTMAN-2, and two Caucasian-based voxel models, Rex and VIP-Man.

2. MATERIALS AND METHODS

2.1. VKH Anatomical Images

HDRK-Man was developed using the color photographic slice images (Fig. 1) from the Visible Korean Human (VKH) project [22]. The images were obtained from the cadaver of a 33-year-old Korean male (164 cm in height and 55 kg in weight) who had died of leukemia. The cadaver was fixed, embedded, and frozen in an immobilization box. It was then serially sectioned in the longitudinal direction at 0.2 mm intervals with a cryomacrotome, and each sectioned surface was photographed with a Kodak DSC560 digital camera providing 3040 $\times$ 2008 pixel resolution (Kodak, Rochester, NY). The images were saved in Tag Image File Format (TIFF) (24 bits color). A total of 8,590 photographic images of 0.1875 mm $\times$ 0.1875 mm resolution were acquired from the cadaver. The color quality and high resolution of the slice images made it possible to accurately segment the organs and tissues, especially the small anatomical structures. The researchers also acquired CT and MR images at 1 mm intervals for possible future use. The major organs and tissues, including the skeleton, lungs, liver, brain, kidneys, skin (external surface), urinary bladder (external surface), heart (internal surface), gastro-intestinal tract (internal surface), main arteries (internal surface), and respiratory tract (internal surface), were segmented by professional anatomists [22].

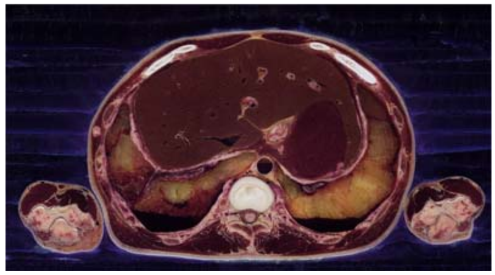

Figure 1. Example of color photographic slice image at mid-level of liver, utilized in model construction

2.2. Segmentation of Organs

Color anatomical images for model construction were selected at every 2 mm interval; that is, 850 images were selected out of the total of 8,590 images. The organs and tissues, clearly distinguished by color, were segmented automatically using Photoshop 7.0 (Abode Systems, Inc., San Jose, CA) and Interactive Data Language (IDL) 5.6. The automatic process was used for the eyes, lenses, skeleton, skin, muscle, colon, small intestine, extrathoracic (ET) region, red bone-marrow, and gall bladder. The other organs, those that could not be segmented automatically, were segmented manually using a screen digitizer CINTIQ 15X (WACOM Co., Ltd, Japan) and the Magnetic Lasso tool in Photoshop 7.0. The Magnetic Lasso tool, which automatically marks the region of selection by identifying differences of color, significantly expedited the segmentation process. The thyroid, urinary bladder, prostate, salivary glands, adrenals, oesophagus, spleen, stomach, lungs, brain, liver, thymus, pancreas, gonads, kidneys, heart, oral mucosa, and blood were segmented manually. The skeleton was divided into nine bone regions [23], and the red bone marrow was segmented considering the distribution of red bone marrow in those regions. After completing the segmentation, the resolution of the segmented images was reduced to 1.875 mm $\times$ 1.875 mm for compatibility with the computation speed and memory size of the computers in use, resulting in an intermediate voxel resolution of 1.875 mm $\times$ 1.875 mm $\times$ 2 mm.

2.3. Adjustment of Height and Skeletal Mass

The body height of the voxel model was adjusted by changing the voxel resolution; that is, the height (164 cm) was matched to the height of the Reference Korean (171 cm) by adjusting the z-resolution from 2 mm to 2.0854 mm. The total skeletal mass was not available in the Reference Korean data and, therefore, it was estimated by the method suggested by Clays *et al*. [14]:

$$m = -10.7 + 0.119 \times HT \quad [kg] \tag{1}$$

where m is the skeletal mass in kg and HT is the height in cm. The height of the Reference Korean is 171 cm, and thus the skeletal mass was calculated as 9.6 kg. The original skeletal mass of 8.6 kg was then matched to 9.6 kg (including red bone marrow) by increasing the in-plane voxel size from 1.875 mm $\times$ 1.875 mm to 1.981 mm $\times$ 1.981 mm. Consequently, the voxel resolution of the final model was 1.981 mm $\times$ 1.981 mm $\times$ 2.0854 mm.

2.4. Adjustment of Individual Organs and Body Weight

The dimensions of the individual organs were adjusted to the Reference Korean data (partially to the Reference Asian data, in the cases of organs and tissues for which Reference Korean data were not available) by utilizing the Inner Grow and Outer Grow functions in Photoshop 7.0. The organs that were larger than those in the Reference Korean data were adjusted by erosion (Inner Grow), and the eroded regions were filled with adipose tissue. The organs smaller than those of the Reference Korean were adjusted by dilation (Outer Grow), adding pixels onto the organ surfaces. The remaining volume in the model, including all of the undefined organs and tissues, was defined as adipose tissue. On completion of the adjustments for the body height, skeletal mass and organ dimensions, the weight of the model was 67.8 kg, which was less than the weight of the Reference Korean (68 kg) by only 0.2 kg. The weight was then adjusted simply by adding 0.2 kg of adipose tissue to the lower parts of the legs. The average tissue compositions and densities in ICRU 46 [24] were used to describe the tissues, except for the lungs and skeleton. The lung density (0.296 g/cm^3) and composition were taken from ICRP 23 [6]. The skeletal density (1.34 g/cm^3) and composition were recalculated from the reference values in ICRP 70 [14] and ICRP 23, respectively, subtracting the elemental composition of red bone marrow, which was explicitly segmented in the present study, from the homogeneous skeletal composition.

2.5. Monte Carlo Organ Dose Calculations

The developed model, HDRK-Man, was implemented into MCNPX [21] for the calculation of the organ absorbed doses. The three-dimensional (3-D) array of the voxel model was converted into a format that can be handled by MCNPX, and the resulting size of the MCNPX input file was about 94 megabytes. The energy deposition tally of track-length estimation, F6, was used to calculate the organ doses. The F6 tally essentially calculates organ-averaged collision kerma in MeV/g per source particle, which was then approximated as an organ-averaged absorbed dose, or organ dose, assuming charged particle equilibrium in all of the organs and tissues of HDRK-Man. The number of source photons transported in the Monte Carlo simulations were 10^8 for 0.015 MeV, 3×10^7 for 0.03-0.05 MeV, and 10^7 for the higher energies. The computation time for each case was 50 – 260 minutes on a HP ProLiant ML570G3 machine equipped with a 3.0 GHz Intel Xeon™ processor and 1024 MB RAM. The statistical errors in the organ doses were less than 5%, except for 0.015 MeV, for which the statistical errors were as large as 100%.

3. RESULTS AND DISCUSSION

The adult Korean male voxel model, HDRK-Man, was constructed from high-resolution photographic anatomical images to represent the average Korean radiation workers. Figure 2 shows 3-D views of the major organs and tissues. The voxel model is 171 cm in height and 68 kg in weight. The size of the voxels (voxel resolution) is $1.981 \times 1.981 \times 2.0854$ mm^3, and the voxel array size is $247 \times 141 \times 850$ (29,602,950) in the x, y, and z directions, which correspond to 489.307 mm, 279.321 mm, and 1,772.59 mm, respectively. The model includes a total of 30 organs and tissues that are required to calculate effective dose.

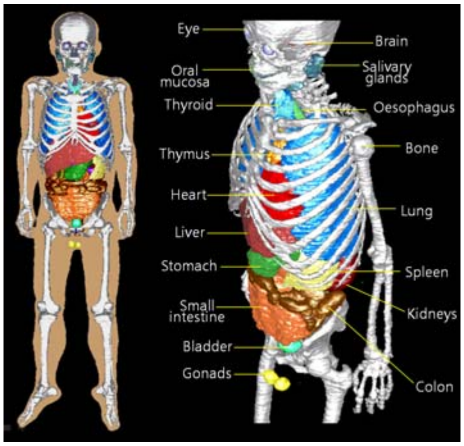

Figure 2. 3-D whole-body frontal view with semi-transparent skin (left) and major organs and tissues (right) of HDRK-Man

Table 1 shows the organ and tissue masses of HDRK-Man along with the reference values used for adjustment. The Reference Asian data [25] were used for the prostate, bladder, adrenals, colon, and small intestines, for which Reference Korean data were not available. The organ masses are in overall good agreement with the Reference Korean data, specifically within 7%, except for the following organs and tissue: the eye lenses were not adjusted due to the limitation of the voxel resolution; the thickness of skin is known to be 1.47 – 2.45 mm [13] but, in the present study, the skin was represented simply by one layer of voxels on the surface of the body; the adipose tissue of HDRK-Man is much heavier than the Reference Korean data, because not only the adipose tissue itself but also all of the undefined organs were defined as adipose tissue.

The dose conversion coefficients, which were organ-averaged absorbed doses per unit air kerma free-in-air (D_T/K_a), calculated by HDRK-Man, were compared with the reported values from other models, KTMAN-2, Rex, and VIP-Man. Four idealized irradiation geometries were compared: antero-posterior (AP), postero-anterior (PA), left-lateral (LLAT), and right- lateral (RLAT). Table 2 shows the dose-conversion coefficients calculated by MCNPX coupled with HDRK-Man.

For a quantitative comparison of the dose conversion coefficients from HDRK-Man with those from the other voxel models, this study defined 'percent dose deviation (δ).' The percent dose deviation, which shows the extent to which a dose conversion coefficient or simply an organ dose calculated by a voxel model deviates from the value calculated from HDRK-Man, is defined as follows for a voxel model, M:

$$\delta = \frac{D_M - D_{HDRK-Man}}{D_{HDRK-Man}} \times 100\% \qquad (2)$$

where D_M and $D_{HDRK\text{-}Man}$ are the dose-conversion coefficients calculated from voxel model M and HDRK-Man, respectively, under identical irradiation conditions. A positive value of δ means that the voxel model M yields a higher dose conversion coefficient than HDRK-Man for a given condition; likewise, a negative value indicates a lower value.

Table I. HDRK-Man organ and tissue masses

Organ	Mass (g) HDRK-Man	Mass (g) Reference Korean	Difference	Organ	Mass (g) HDRK-Man	Mass (g) Reference Korean	Difference
Bone	9607	9649	-0.4%	Small intestine	602	590[a]	2.0%
Liver	1474	1438	2.5%	Oesophagus	40	40	0.0%
Lungs	1156	1123	2.9%	Adrenals	14	14[a]	0.0%
Brain	1620	1522	6.4%	Skin	4260	2400	77.5%
Kidneys	359	338	6.2%	Extrathoracic region	73	-	-
Spleen	177	170	4.1%	Thyroid	15	15	0.0%
Stomach	141	140	0.7%	Bone-marrow (red)	1068	1000	6.8%
Pancreas	126	130	-3.1%	Prostate	12	12[a]	0.0%
Thymus	39	40	-2.5%	Blood	254	-	-
Gonads	28	29	-3.4%	Salivary glands	87	82	6.1%
Eyes	21	20	5.0%	Gall bladder	13	13	0.0%
Lens	0.51	0.4	27.5%	Oral mucosa	21	-	-
Muscle	23300	25000	-6.8%	Heart wall	391	380	2.9%
Bladder	42	40[a]	5.0%	Breast	23.3	22	5.9%
Colon	343	330[a]	3.9%	Adipose tissue	23400.2	11000	112.7%

[a] The Reference Asian data were used for the organs and tissues for which Reference Korean data were not available.

Figure 3 shows the distribution of δ for KTMAN-2, Rex, and VIP-Man, for a total of 44 irradiation conditions and 11 organs (i.e., $44 \times 11 = 484$ cases) - that is, 4 irradiation geometries (AP, PA, RLAT, and LLAT), 11 photon energies (0.03, 0.04, 0.05, 0.08, 0.2, 0.4, 0.6, 0.8, 2, 8, and 10 MeV), and 11 major organs and tissues (i.e., gonads, red bone-marrow, colon, lung, stomach, bladder, liver, oesophagus, thyroid, skin, and bone surface) for which the organ dose values are available for all of the voxel models considered in the present study. The results show that KTMAN-2, Rex, and VIP-Man tend to yield lower dose conversion coefficients than HDRK-Man, which is reasonable considering that HDRK-Man is smaller than the other models, especially in the torso, resulting in less shielding for the internal organs. The average ($\bar{\delta}$) of the percent dose deviations were calculated as -7%, -11%, and -17% for KTMAN-2, Rex, and VIP-Man, respectively. The largest deviation was observed for VIP-Man, which is significantly heavier than HDRK-Man. Even though KTMAN-2 and HDRK-Man have similar heights and weights, KTMAN-2 tends to yield somewhat lower values than HDRK-Man, due to the facts that (1) HDRK-Man has a smaller torso than KTMAN-2, and (2) the arms of HDRK-Man are shifted backward, meaning that the internal organs positioned mainly in the torso region are less shielded from radiation in RLAT and LLAT geometries. Nevertheless, KTMAN-2 showed the best agreement with HDRK-Man, which was expected, as they represent the same racial group. The discrepancy of the dose conversion coefficients between these two models was less than 20% for 75% of a total of 484 irradiation cases. The discrepancy exceeded 50% only for 6% of the total cases.

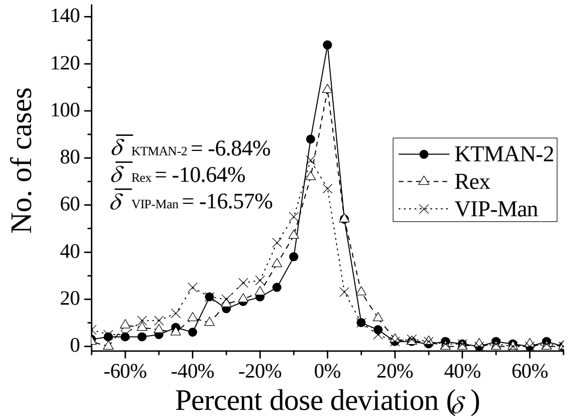

Figure 3. Distribution of percent dose deviations (δ) calculated between three reference voxel models and HDRK-Man

4. CONCLUSIONS

In the present study, a Korean adult male voxel model, called HDRK-Man, was constructed using high-resolution color photographic slice images of a Korean adult male cadaver. The model dimensions, including the body height and weight, the skeletal mass, and the dimensions of the individual organs, were matched to the Reference Korean data. The resulting model was then implemented into MCNPX to calculate the dose conversion coefficients, which were found to be reasonable when compared with the values from the other adult voxel models. HDRK-Man, which is 171 cm in height and 68 kg in weight and has organs and tissues of Reference Korean size, is believed to adequately represent the average Korean workers and thus can be used for more accurate calculation of dose conversion coefficients for the Korean workers in the future. It should be emphasized, however, that the current version of HDRK-Man, with its Reference Korean-adjusted dimensions, was developed for radiation protection purposes only, and therefore cannot be used in medical applications for which more precise representation of a human body is necessary. In these latter cases, one can use the unadjusted version of HDRK-Man instead. The voxel resolution of HDRK-Man is currently $1.981 \times 1.981 \times 2.0854$ mm^3, which is adequate for average organ dose calculations for radiation protection purposes. The resolution of the model, however, can be enhanced to $0.1981 \times 0.1981 \times 0.20854$ mm^3 for any sub-region of the model. For example, it is easy to develop a voxel model that has $0.1981 \times 0.1981 \times 0.20854$ mm^3 voxel resolution for the eye region, but with $1.981 \times 1.981 \times 2.0854$ mm^3 voxel resolution for the other regions of the body. This kind of model could be used to calculate very detailed dose distributions in the eye region without significantly affecting the computation speed or memory requirement.

ACKNOWLEDGMENTS

This work was supported by the Korean Ministry of Science and Technology (MOST) through the Korea Institute of Nuclear Safety (KINS), ERC (RII-2000-067-03002-0), and BAERI (M20508050003-05B0805-00310).

Table II. Dose conversion coefficients calculated from HDRK-Man

Energy (MeV)	AP	PA	RLAT	LLAT	AP	PA	RLAT	LLAT	AP	PA	RLAT	LLAT
	Bladder				Bone-marrow (red)				Bone			
0.015	0.002	-	-	-	0.003	0.003	0.002	0.002	0.032	0.016	0.016	0.016
0.030	0.369	0.091	0.017	0.019	0.131	0.182	0.066	0.067	0.866	0.691	0.484	0.488
0.040	0.817	0.319	0.087	0.100	0.339	0.466	0.176	0.177	1.822	1.598	1.029	1.030
0.050	1.189	0.573	0.202	0.225	0.570	0.759	0.303	0.304	2.511	2.295	1.445	1.440
0.080	1.527	0.911	0.416	0.448	0.911	1.156	0.512	0.512	2.457	2.335	1.457	1.454
0.200	1.228	0.854	0.447	0.485	0.880	1.070	0.534	0.535	1.195	1.148	0.755	0.754
0.400	1.093	0.845	0.511	0.538	0.851	0.996	0.557	0.555	0.993	0.956	0.668	0.667
0.600	1.057	0.824	0.550	0.583	0.851	0.974	0.583	0.582	0.955	0.924	0.670	0.668
0.800	1.040	0.842	0.582	0.631	0.861	0.968	0.611	0.610	0.947	0.919	0.684	0.683
2.000	1.006	0.898	0.723	0.736	0.896	0.970	0.712	0.711	0.948	0.930	0.756	0.755
8.000	0.999	0.935	0.843	0.852	0.929	0.971	0.818	0.818	0.994	0.982	0.874	0.873
10.000	0.996	0.934	0.846	0.854	0.930	0.969	0.825	0.824	1.004	0.993	0.890	0.889
	Brain				Breast				Colon			
0.015	-	-	-	-	0.410	-	0.050	0.038	0.014	-	0.001	0.001
0.030	0.127	0.136	0.159	0.154	0.806	0.008	0.300	0.253	0.431	0.155	0.172	0.142
0.040	0.381	0.417	0.450	0.440	1.015	0.045	0.425	0.368	0.853	0.424	0.372	0.329
0.050	0.630	0.682	0.719	0.701	1.233	0.104	0.550	0.485	1.191	0.697	0.550	0.499
0.080	0.903	0.947	0.984	0.972	1.577	0.251	0.789	0.705	1.482	1.033	0.741	0.696
0.200	0.813	0.843	0.870	0.862	1.481	0.394	0.897	0.808	1.177	0.909	0.672	0.637
0.400	0.801	0.826	0.850	0.842	1.339	0.494	0.918	0.842	1.061	0.864	0.677	0.643
0.600	0.815	0.837	0.857	0.850	1.276	0.564	0.928	0.861	1.028	0.860	0.698	0.667
0.800	0.829	0.851	0.868	0.865	1.245	0.616	0.940	0.879	1.013	0.865	0.719	0.692
2.000	0.891	0.904	0.915	0.912	1.177	0.765	0.986	0.947	0.997	0.898	0.798	0.782
8.000	0.938	0.943	0.949	0.948	1.092	0.852	0.982	0.960	0.989	0.926	0.877	0.865
10.000	0.939	0.943	0.949	0.948	1.077	0.848	0.974	0.951	0.985	0.926	0.880	0.868
	Gonads				Liver				Lungs			
0.015	0.123	0.009	0.005	-	0.004	-	-	-	0.001	0.001	0.001	0.001
0.030	1.022	0.156	0.094	0.053	0.338	0.067	0.169	0.041	0.238	0.267	0.156	0.120
0.040	1.462	0.363	0.209	0.158	0.795	0.258	0.464	0.156	0.595	0.654	0.363	0.286
0.050	1.749	0.551	0.318	0.268	1.192	0.491	0.746	0.295	0.910	0.991	0.553	0.447
0.080	1.835	0.787	0.458	0.410	1.550	0.814	1.027	0.488	1.221	1.322	0.755	0.631
0.200	1.431	0.722	0.490	0.443	1.175	0.722	0.867	0.475	1.000	1.099	0.667	0.573
0.400	1.248	0.782	0.549	0.506	1.044	0.715	0.833	0.511	0.934	1.021	0.669	0.589
0.600	1.190	0.802	0.598	0.561	1.007	0.730	0.837	0.548	0.923	0.999	0.690	0.620
0.800	1.159	0.818	0.634	0.595	0.995	0.751	0.848	0.583	0.925	0.994	0.716	0.650
2.000	1.091	0.887	0.751	0.730	0.982	0.820	0.895	0.704	0.946	0.994	0.802	0.755
8.000	1.048	0.923	0.847	0.843	0.981	0.881	0.936	0.821	0.965	0.989	0.882	0.855
10.000	1.043	0.921	0.855	0.852	0.979	0.882	0.935	0.828	0.964	0.986	0.887	0.860
	Oesophagus				Salivary glands				Skin			
0.015	-	-	-	-	0.006	0.008	0.049	0.059	0.373	0.359	0.218	0.217
0.030	0.135	0.066	0.043	0.062	0.272	0.311	0.393	0.440	0.700	0.675	0.448	0.447
0.040	0.434	0.316	0.176	0.237	0.552	0.577	0.630	0.687	0.876	0.850	0.570	0.570
0.050	0.752	0.619	0.352	0.434	0.794	0.798	0.826	0.888	1.012	0.985	0.664	0.664
0.080	1.161	1.060	0.587	0.705	1.059	1.048	1.025	1.103	1.139	1.109	0.763	0.763
0.200	0.936	0.899	0.603	0.661	0.989	1.001	0.937	0.979	1.044	1.016	0.744	0.744
0.400	0.883	0.848	0.627	0.682	0.965	0.982	0.901	0.938	1.004	0.979	0.752	0.753
0.600	0.877	0.841	0.661	0.714	0.953	0.982	0.898	0.929	0.995	0.972	0.769	0.770
0.800	0.877	0.845	0.699	0.736	0.959	0.985	0.903	0.935	0.995	0.974	0.786	0.788
2.000	0.900	0.886	0.804	0.828	0.985	1.003	0.935	0.952	1.001	0.986	0.848	0.850
8.000	0.923	0.912	0.872	0.887	0.984	0.985	0.951	0.956	0.995	0.987	0.906	0.909
10.000	0.924	0.912	0.873	0.888	0.978	0.980	0.951	0.955	0.992	0.984	0.908	0.911

Table II. Dose conversion coefficients calculated from HDRK-Man (continued)

Energy (MeV)	AP	PA	RLAT	LLAT	AP	PA	RLAT	LLAT	AP	PA	RLAT	LLAT
	Stomach				Thyroid				Adrenals			
0.015	0.020	-	-	-	0.061	-	0.001	-	-	-	-	-
0.030	0.538	0.032	0.073	0.161	0.918	0.028	0.191	0.158	0.084	0.124	0.020	0.033
0.040	1.005	0.168	0.210	0.443	1.505	0.179	0.483	0.427	0.318	0.436	0.112	0.149
0.050	1.378	0.359	0.351	0.694	1.907	0.426	0.742	0.682	0.595	0.781	0.256	0.306
0.080	1.699	0.671	0.543	0.961	2.134	0.731	0.975	0.953	0.996	1.228	0.474	0.531
0.200	1.284	0.638	0.544	0.843	1.539	0.669	0.832	0.817	0.888	1.059	0.499	0.538
0.400	1.144	0.648	0.582	0.837	1.327	0.677	0.833	0.823	0.846	0.988	0.519	0.571
0.600	1.095	0.676	0.618	0.850	1.250	0.696	0.857	0.849	0.846	0.954	0.544	0.584
0.800	1.074	0.702	0.654	0.866	1.221	0.719	0.881	0.876	0.863	0.948	0.576	0.612
2.000	1.041	0.782	0.767	0.917	1.146	0.822	0.946	0.949	0.896	0.948	0.696	0.720
8.000	1.022	0.867	0.865	0.955	1.096	0.905	0.971	0.971	0.925	0.958	0.809	0.818
10.000	1.019	0.869	0.870	0.954	1.089	0.907	0.968	0.968	0.929	0.958	0.810	0.829
	Blood				Extrathoracic region				Gall bladder			
0.015	0.002	-	-	-	0.042	-	-	0.012	0.004	-	-	-
0.030	0.179	0.095	0.059	0.096	0.507	0.020	0.222	0.240	0.418	0.034	0.199	0.024
0.040	0.542	0.361	0.223	0.325	0.893	0.116	0.500	0.520	0.886	0.181	0.531	0.101
0.050	0.912	0.670	0.411	0.564	1.206	0.257	0.761	0.778	1.260	0.381	0.813	0.198
0.080	1.291	1.074	0.656	0.847	1.488	0.501	1.058	1.076	1.630	0.699	1.132	0.370
0.200	1.013	0.894	0.627	0.745	1.253	0.552	1.000	1.009	1.246	0.691	0.963	0.405
0.400	0.914	0.832	0.655	0.749	1.137	0.603	0.969	0.983	1.117	0.701	0.924	0.471
0.600	0.898	0.828	0.693	0.772	1.099	0.650	0.970	0.977	1.070	0.711	0.923	0.507
0.800	0.895	0.836	0.727	0.796	1.080	0.674	0.975	0.980	1.053	0.730	0.924	0.556
2.000	0.913	0.872	0.823	0.865	1.052	0.781	0.989	0.991	1.014	0.809	0.949	0.697
8.000	0.941	0.914	0.899	0.924	1.029	0.870	0.994	0.995	1.001	0.881	0.953	0.801
10.000	0.942	0.917	0.902	0.926	1.025	0.872	0.992	0.992	0.996	0.880	0.947	0.805
	Heart				Kidneys				Muscle			
0.015	0.001	-	-	-	-	0.002	-	-	0.036	0.038	0.018	0.018
0.030	0.247	0.052	0.065	0.137	0.080	0.370	0.039	0.057	0.393	0.492	0.208	0.203
0.040	0.697	0.232	0.235	0.402	0.305	0.856	0.147	0.203	0.693	0.845	0.375	0.367
0.050	1.119	0.461	0.423	0.663	0.557	1.256	0.279	0.361	0.938	1.112	0.517	0.506
0.080	1.506	0.791	0.669	0.947	0.886	1.611	0.468	0.568	1.164	1.323	0.659	0.648
0.200	1.168	0.720	0.652	0.831	0.768	1.252	0.426	0.500	1.002	1.101	0.603	0.593
0.400	1.033	0.711	0.683	0.815	0.741	1.110	0.442	0.508	0.951	1.020	0.610	0.602
0.600	0.999	0.730	0.717	0.827	0.757	1.059	0.469	0.529	0.942	0.998	0.631	0.624
0.800	0.989	0.747	0.749	0.841	0.769	1.042	0.497	0.557	0.944	0.993	0.654	0.648
2.000	0.978	0.818	0.841	0.891	0.837	1.015	0.620	0.670	0.960	0.992	0.743	0.739
8.000	0.980	0.880	0.902	0.930	0.895	0.999	0.759	0.798	0.971	0.991	0.842	0.840
10.000	0.978	0.883	0.902	0.931	0.896	0.996	0.770	0.804	0.969	0.989	0.849	0.846
	Oral mucosa				Pancreas				Prostate			
0.015	0.073	-	0.015	0.017	0.002	-	-	-	-	-	-	-
0.030	0.517	0.019	0.282	0.294	0.353	0.033	0.034	0.080	0.141	0.198	0.008	0.010
0.040	0.842	0.103	0.546	0.559	0.812	0.191	0.158	0.282	0.500	0.531	0.065	0.070
0.050	1.106	0.231	0.789	0.800	1.211	0.418	0.315	0.501	0.870	0.851	0.165	0.184
0.080	1.394	0.458	1.075	1.089	1.588	0.801	0.552	0.778	1.225	1.211	0.364	0.379
0.200	1.219	0.526	1.029	1.037	1.238	0.736	0.538	0.697	1.053	1.002	0.382	0.421
0.400	1.111	0.587	1.005	0.992	1.103	0.729	0.557	0.708	0.935	0.951	0.445	0.467
0.600	1.080	0.635	0.988	0.989	1.065	0.740	0.591	0.728	0.938	0.921	0.461	0.507
0.800	1.059	0.671	0.990	0.990	1.045	0.758	0.630	0.755	0.940	0.938	0.488	0.539
2.000	1.032	0.768	0.994	0.988	1.021	0.823	0.744	0.837	0.950	0.930	0.642	0.667
8.000	0.997	0.835	0.974	0.973	1.002	0.878	0.841	0.893	0.944	0.921	0.787	0.814
10.000	0.992	0.836	0.968	0.966	0.998	0.879	0.842	0.893	0.943	0.919	0.800	0.818

Table II. Dose conversion coefficients calculated from HDRK-Man (continued)

Energy (MeV)	Small intestine AP	Small intestine PA	Small intestine RLAT	Small intestine LLAT	Spleen AP	Spleen PA	Spleen RLAT	Spleen LLAT	Thymus AP	Thymus PA	Thymus RLAT	Thymus LLAT
0.015	0.025	-	0.001	0.001	0.001	-	-	0.001	0.002	-	-	-
0.030	0.612	0.028	0.112	0.108	0.262	0.134	0.005	0.382	0.396	0.019	0.051	0.085
0.040	1.111	0.163	0.299	0.286	0.670	0.438	0.039	0.853	0.918	0.121	0.212	0.292
0.050	1.483	0.364	0.480	0.460	1.027	0.747	0.100	1.233	1.326	0.285	0.381	0.503
0.080	1.754	0.699	0.699	0.670	1.323	1.108	0.224	1.503	1.691	0.552	0.619	0.774
0.200	1.336	0.680	0.666	0.639	1.029	0.920	0.249	1.172	1.334	0.552	0.631	0.743
0.400	1.171	0.688	0.685	0.670	0.936	0.863	0.304	1.065	1.181	0.559	0.661	0.750
0.600	1.113	0.710	0.714	0.701	0.924	0.851	0.353	1.044	1.117	0.594	0.699	0.783
0.800	1.089	0.734	0.742	0.728	0.918	0.858	0.398	1.035	1.091	0.619	0.730	0.802
2.000	1.045	0.808	0.828	0.817	0.940	0.893	0.567	1.028	1.047	0.716	0.821	0.868
8.000	1.016	0.870	0.891	0.886	0.950	0.918	0.740	1.014	1.016	0.817	0.887	0.918
10.000	1.012	0.873	0.893	0.889	0.949	0.918	0.751	1.011	1.011	0.826	0.890	0.921

REFERENCES

1. International Commission on Radiation Units and Measurements, *Phantoms and Computational Models in Therapy*, *Diagnosis and Protection*, ICRU report 48, ICRU, Bethesda U.S.A.(1992).
2. H. L. J. Fisher, and W. S. Snyder, *Distribution of Dose in the Body from a Source of Gamma Rays Distributed Uniformly in an Organ*, ORNL-4168, Oak Ridge National Laboratory, Oak Ridge U.S.A. (1967).
3. M. Cristy, and K. F. Eckerman, *Specific Absorbed Fractions of Energy at Various Ages from Internal Photon Sources*, ORNL/TM-8381, Oak Ridge National Laboratory, Oak Ridge U.S.A. (1987).
4. R. Kramer, M. Zankl, G. Williams, and G. Drexler, *The Calculation of Dose from External Photon Exposures Using Reference Human Phantoms and Monte-Carlo Methods, Part 1: The Male (ADAM) and Female (EVA) Adult Mathematical Phantoms*, GSF Bericht S-885, GSF-National Research Center for Health and Environment, Neuherberg Germany (1982).
5. M. G. Stabin, E. Watson and M. Cristy. "Mathematical Models and Specific Absorbed Fractions of Photon Energy in the Nonpregnant Adult Female and at the End of Each Trimester of Pregnancy," ORNL/TM-12907, Oak Ridge National Laboratory, Oak Ridge U.S.A. (1995).
6. International Commission on Radiological Protection, *Reference Man: Anatomical, Physiological and Metabolic Characteristics*, ICRP Publication 23, Pergamon Press, Oxford U.K. (1975).
7. International Commission on Radiological Protection, *Recommendation of the International Commission on Radiological Protection*, ICRP DRAFT 2007 (2007).
8. S. J. Gibbs, A. Pujol, T. S. Chen, and A. W. Malcolm, "Computer-Simulation of Patient Dose from Dental Radiography," *J. Dent. Res.*, **Vol. 63**, pp.209 (1984).
9. I. G. Zubal, C. R. Harrell, E. O. Smith, Z. Rattner, G. Gindi, and P. B. Hoffer, "Computerized Three-dimensional Segmented Human Anatomy," *Med. Phys.*, **Vol. 21**, pp.299-302 (1994).

10. P. J. Dimbylow, “The Development of Realistic Voxel Phantoms for Electromagnetic Field Dosimetry,” *Proceedings of an International Workshop at the National Radiological Protection Board*, Chilton U.K., July 6-7 (1995)
11. M. Zankl, J. Becker, U. Fill, N. Petoussi-Henss, and KF. Eckerman, “GSF Male and Female Adult Voxel Models Representing ICRP Reference Man - The Present Status”, *Proceeding of The Monte Carlo Method: Versatility Unbounded in a Dynamic Computing World*, Chattanooga U.S.A., April 17-21 (2005).
12. H. Schlattl, M. Zankl, and N. Petoussi-Henss, “Organ Dose Conversion Coefficients for Voxel Models of the Reference Male and Female from Idealized Photon Exposures,” *Phys. Med. Biol.*, **Vol. 52**, pp.2123-2145 (2007).
13. International Commission on Radiological Protection, *Basic Anatomical and Physiological Data for use in Radiological Protection: Reference Values*, ICRP Publication 89, Pergamon Press, Oxford U.K. (2002).
14. International Commission on Radiological Protection, *Basic Anatomical and Physiological Data for use in Radiological Protection: The Skeleton*, ICRP Publication 70, Pergamon Press, Oxford U.K. (1994).
15. K. Saito, A. Wittmann, S. Koga, Y. Ida, T. Kamei, J. Funabiki, and M. Zankl, “Construction of a Computed Tomographic Phantom for a Japanese Male Adult and Dose Calculation System,” *Radiat. Environ. Biophys.*, **Vol. 40,** pp.69-76 (2001).
16. G. Tanaka, Y. Nakahara, and Y. Nakazima, “Japanese Reference Man 1988-IV. Studies on the Weight and Size of Internal Organs of Normal Japanese,” *Nippon Igaku Hoshasen Gakkai Zasshi*, **Vol. 49**, pp.344-364 (1989).
17. C. Lee, J. Lee, “Computational Anthropomorphic Phantoms for Radiation Protection Dosimetry: Evolution and Prospects,” *Nucl. Eng. Technol.*, **Vol. 38**, pp.239-250 (2006).
18. S. Park, J. Lee, J. I. Kim, Y. J. Lee, Y. K. Lim, C. S. Kim, and C. Lee, “In Vivo Organ Mass of Korean Adults Obtained from Whole-body Magnetic Resonance Data,” *Radiat. Prot. Dosim.*, **Vol. 118**, pp.275-279 (2005).
19. M. Caon, "Voxel-based Computational Models of Real Human Anatomy: a Review," *Radiat. Environ. Biophys.*, **Vol. 42**, pp.229-235 (2004).
20. X. G. Xu, T. C. Chao, and A. Bozkurt, "VIP-MAN: An Image-based Whole-body Adult Male Model Constructed from Color Photographs of the Visible Human Project for Multi-particle Monte Carlo Calculations," *Health Phys.*, **Vol. 78**, pp.476-486 (2000).
21. D. B. Pelowitz, *MCNPX User’s Manual Version 2.5.0*, LA-CP-05-0369, Los Alamos National Laboratory, Los Alamos U.S.A. (2005).
22. J. S. Park, M. S. Chung, J. Y. Kim, and H. S. Park, “Visible Korean Human: Another Ttrial for making Serially Sectioned Images,” *SPIE Med. Imaging*, **Vol. 4681**, pp.171-183 (2002).
23. R. Kramer, J. W. Vieira, H. J. Khoury, F. R. A. Lima, and D. Fuelle, “All about MAX: a Male Adult Voxel Phantom for Monte Carlo Calculations in Radiation Protection Dosimetry,” *Phys. Med. Biol*. **Vol. 48**, pp.1239-1262 (2003).
24. International Commission on Radiation Units and Measurements, *Photon, Electron, Proton and Neutron Interaction Data for Body Tissues*, ICRU Report 46, ICRU, Bethesda U.S.A. (1992).
25. International Atomic Energy Agency, *Compilation of anatomical, physiological and metabolic characteristics for a Reference Asian Man*, IAEA-TECDOC-1005, Vienna Austria (1998).